Competition between generic and nongeneric fronts in envelope equations

James A. Powell* and Alan C. Newell
Department of Mathematics, University of Arizona, Tucson, Arizona 85721

Christopher K. R. T. Jones
Division of Applied Math, Brown University, Providence, Rhode Island 02912
(Received 1 March 1990; revised manuscript received 21 January 1991)

Arguments are presented for understanding the selection of the speed and the nature of the fronts that join stable and unstable states on the supercritical side of first-order phase transitions. It is suggested that from compact support, nonpositive-definite initial conditions, observable front behavior occurs only when the asymptotic spatial structure of a trajectory in the Galilean ordinary differential equation (ODE) corresponds to the most unstable temporal mode in the governing partial differential equation (PDE). This selection criterion distinguishes between a "nonlinear" front, which has its origin in the first-order nature of the bifurcation, and a "linear" front. The nonlinear front has special properties as a strongly heteroclinic trajectory in the ODE and as an integrable trajectory in the PDE. Many of the characteristics of the linear front are obtained from a steepest-descent linear analysis originally due to Kolmogorov, Petrovsky, and Piscounov [Bull. Univ. Moscow, Ser. Int., Sec. A **1**, 1 (1937)]. Its connection with global stability arguments, and in particular with arguments based on a Lyapunov functional where it exists, is pursued. Finally, the point of view and results are compared and contrasted with those of van Saarloos [Phys. Rev. A **37**, 211 (1988); **39**, 6367 (1989)].

I. INTRODUCTION

Fronts in reaction-diffusion partial differential equations (PDE's) have received the interest of both mathematicians and physical scientists. A front is a propagating interface between two different steady states and can be viewed physically as a balance between diffusive forces coupling different points in the field, and reactive forces which move the system from unstable to stable states. Fronts are relevant in optical, chemical, hydrodynamic, and biological fields, which is why they have received so much attention from the applied-mathematical community.

Perhaps the beginning of rigorous interest in fronts was due to the Fisher-Kolmogorov (FK) equation

$$u_t = u_{xx} + u - u^3 , \tag{1}$$

which arose in population dynamics. This equation exhibits several characteristics relevant to the rest of this paper: an unstable uniform state ($u=0$), stable uniform states ($u=\pm 1$), second-order diffusion, and first-order time derivatives. Fronts that oscillate about zero exist in the FK equation, but they were viewed as unphysical since they represent negative population densities. Consequently, interest was focused on strictly non-negative solutions, which is consistent since positive solutions must stay positive in an equation like (1). However, in some kinds of physical problems there is no reason to restrict ourselves to positive solutions. In fact, in hydrodynamic types of problems we may wish to allow oscillatory perturbations to the unstable state and see what role the oscillatory fronts play. We will show later that although the oscillatory fronts are not stable, they do play an important dynamical role.

Fronts in the FK equation connect the unstable to the stable state, and move in such a way as to destabilize the unstable state. The preferred front speed is the speed at which an observer must move in order to see local exponential growth of the most unstable perturbations as stationary in his frame of reference. It is the speed of a surfer on a wave which seems to be growing to a stationary observer. With this sort of intuition, Kolmogorov, Petrovsky, and Piscounov [1] were able to use a method of stationary phase and steepest descent to find the asymptotic speed of fronts in Eq. (1).

Equation (1) is the real version of either complex Ginzburg-Landau (GGL) [2–4] or Newell-Whitehead-Segel (NWS) [5,6] equations. These are envelope equations that describe the dynamics of wave envelopes near transition in hydrodynamic systems. The CGL equation, which describes the evolution of a traveling-wave envelope written in a frame of reference traveling with the group velocity of the underlying carrier wave, may be written

$$A_t = A + (1+i\beta)A_{xx} - (1+i\gamma)A|A|^2 , \tag{2}$$

and the NWS equation is (2) with β and γ set to zero, corresponding to a situation in which exchange of stabilities occurs and the new state is fixed in space. For both of these equations, and consequently for the FK equation, Dee and Langer [7] showed that Kolmogorov's approach is equivalent to finding the maximal speed of unstable Fourier modes in the linear portion of (2). The idea is that a perturbation about the unstable state is a sum of Fourier modes, each of which obeys the linear dispersion relation of (2). Given an initial perturbation with compact support, the far field will first be destabilized by the most rapidly growing mode. This critical mode will then

determine the subsequent growth of the asymptotic front.

Dee and Langer observe that their approach is equivalent to a marginal stability approach used by Fisher in the FK equation [8]. Marginality, they point out, means that the asymptotic front speed and the group velocity are the same. Hence the marginal front should be stable; neutrally stable perturbations move at the group velocity and do not change the marginal front. Perturbations that do grow move more slowly and must therefore be outrun by the marginal front. The asymptotic speed of the stable front should therefore be given by the marginal front speed.

Numerical results, for example those of Nozaki and Bekki [9], indicate that the marginal stability approach gives the speed of the preferred fronts in the FK, CGL, and NWS equations. However, in all of these equations the phase transition is in second order and the relative strength of the nonlinearity is fixed. In equations that allow for tuning the relative strength of competing nonlinear contributions, Aronson and Weinberger [10] calculated explicit fronts which propagate at speeds *faster* than the supposedly maximal marginal speed. One equation for which this occurs is

$$u_t = u_{xx} + \frac{u}{b}(b+u)(1-u) \ . \tag{3}$$

Equation (3) was studied extensively by Ben-Jacob *et al.* [11], and the results were summarized by van Saarloos [12,13]. The parameter b adjusts the relative strengths of second- and third-order nonlinearities in (3). For some parameter regimes, the marginal front is shown to be unstable to an "isolated nonlinear mode" of the PDE. This special solution has asymptotic behavior which corresponds to a discrete point in the normally continuous spectrum of possible asymptotic speeds. When this discrete speed describes a front with steeper asymptotic decrease than the marginal front, it is the asymptotic speed for fronts in (3).

van Saarloos [12,13] showed that similar circumstances exist in other systems where the relative strengths of nonlinearities can be changed. In the equation

$$u_t = u + u_{xx} + du^3 - u^5 \tag{4}$$

he showed that in precisely determined parameter regimes a special "nonlinear" speed is preferred over the marginal speed. He also showed that the approach to the asymptotic speed is exponential in the case of nonlinear preference, but only algebraic in the case of linear marginal preference. Essential to van Saarloos's argument is the analysis of the linear dispersion relation

$$\lambda^2 + c\lambda + 1 = 0 \tag{5}$$

of neutral modes $e^{\lambda(x-ct)}$ in the linear portion of (4). Earlier work by Ben-Jacob and others [1,2] shows that the nonoscillatory fronts are stable to perturbations which decay more rapidly than the front itself, and have asymptotic behavior determined (generically) by the smaller of the roots of (5). The exception to this rule is the special nonlinear front with nongeneric asymptotic behavior, which is stable, but has more rapid decay to zero. Since greater front speed results in a more leisurely approach to zero and consequently stability to a broader set of initial conditions, one might infer that the more rapid the front the more stable it is. These earlier authors also show that oscillatory fronts are unstable. Moreover, since they are considering the evolution of strictly non-negative initial conditions, the fact that positive solutions remain positive strictly precludes oscillatory fronts from playing any dynamic role whatsoever. By comparing the asymptotic spatial decay of the strictly positive fronts, van Saarloos concludes that in some regimes the special nonlinear solution is the asymptotic front state, while in other the slowest nonoscillatory front, a linear Kolmogorov-Langer front is preferred.

In this paper we will depart from the work of earlier authors by allowing solutions to be negative. In fact, even when the initial conditions are strictly non-negative, we will allow oscillatory perturbations to influence the development of the fronts. The idea is to model random oscillatory perturbations as a front develops in a hydrodynamic context, and with this change in approach we find an important result. The asymptotic behavior suggested by the ordinary differential equation (ODE) dynamics is not accessible behavior in the PDE; that is, from compact support initial conditions solutions do not seem to approach any of the "stable," nonoscillatory fronts except either the linear or nonlinear fronts. This may be due to the fact that truncating these stable fronts is really perturbing them with a function that does not decay more quickly than the front itself, and so the stability results of Ben-Jacobs are inappropriate for compact support initial conditions. In the presence of ongoing oscillatory perturbations, we suggest that the only front solutions of the PDE accessible from compact support initial conditions are a continuum of unstable modes with speeds $0 < c \leq c^*$ and a single nonlinear mode with speed $\tilde{c}$. These modes, except for $c = c^*$ and $c = \tilde{c}$, correspond to fronts with oscillatory spatial structure that are unstable. However, we will demonstrate that oscillating fronts appear transiently as fronts converge to the asymptotic states.

Nonoscillatory fronts with $c > c^*$, solutions of the ODE which play a major role in determining the asymptotic behavior of strictly positive initial conditions, are irrelevant because they play no part in the dynamics of front convergence when oscillatory perturbations are present. By "relevant" we mean a front that is observed either as a transient or an asymptotic state, and we suggest relevant front behavior occurs when the solutions allowed by both the PDE and the ODE concur. The contention that oscillatory fronts are relevant and "accessible" is based on numerical simulations in which we start with a variety of ODE front solutions, truncated in their tails, and examine how they evolve to their asymptotic states. In particular we measure the distance between transients and oscillatory fronts numerically and show that it is small. We support these ideas by considering the dynamics of the Liapunov functional for the real equation, but stress that this is not a proof but a heuristic argument. However, there is no doubt that dynamic competition between fronts from these initial conditions

favors the oscillatory fronts, even though they are not stable in the usual sense.

We also introduce the idea, unproven in general but valid in every case tested, that the nonlinear solutions can be determined using the Weiss, Tabor, and Carnevale (WTC) method. The WTC method was originally developed to reveal the potential integrability of systems of PDE's by investigating whether the general solution has the strong or weak Painlevé property. Truncating the Painlevé series gives rise to an overdetermined set of equations whose solutions, when they exist, have very special properties. In a recent paper, Cariello and Tabor [14] showed that, even though the original equations are not in general integrable, certain solutions of the original PDE can be found by using the same overdetermined systems arising from the truncated Painlevé expansion. Our observation was that these special solutions always corresponded to special heteroclinic orbits, and they appear to capture all the relevant nonlinear front solutions. Although we do not yet fully understand the reason for this remarkable property, the observation gives a mathematical framework in which van Saarloos's reduction of order ansatz for finding the nonlinear solutions may be understood in terms of analytical properties. Accordingly, we show that the WTC method gives a reduction of order in a traveling frame of reference.

We transform Eq. (4) into a form familiar in that context,

$$u_t=\mu u+u_{xx}+u^3-u^5 , \tag{6}$$

by rescaling t, x, and u. In this form μ plays the role of a scaled stress parameter near a subcritical bifurcation from an unstable state, e.g., Rayleigh number in binary convection or Reynolds number in Taylor-Couette flow. Equation (6) is in a form reminiscent of amplitude equations for such subcritical bifurcations. It is also the real version of a model CGL-type equation many authors have used to begin describing nonlinear phenomena arising in these circumstances,

$$A_t=\mu A+(1+i\beta)A_{xx}+(1+i\gamma)A|A|^2-(1+i\delta)A|A|^4 . \tag{7}$$

Jones, Kapitula, and Powell [15] have discussed the parametrization and existence of subcritical fronts in (7). They show that there is in fact only one stable front for most of the subcritical regime. WTC solutions exist for (7) in both subcritical and supercritical regimes, and are a continuous deformation of the unique subcritical fronts described by Jones, Kapitula, and Powell. We will present results for (7), but will focus the paper on (6), where the details of the calculations are mathematically, pictorially, and intuitively clear.

By way of introduction to Eq. (6) we will first apply the Kolmogorov method of stationary phases to determine the linear marginal speed in Sec. II. Although this only gives a leading-order approximation for the linear front, it illustrates the special role of marginal front speed and leads naturally to Langer's marginality idea [5]. In Sec. III we will use the WTC method to find special fronts and show that these are equivalent to the fronts found using van Saarloos's "reduction of order." In Sec. IV we will find the continuum of accessible front speeds and present a unified understanding of the spatial structure of the linear and nonlinear solutions using phase-space arguments. The correspondence of stability, integrability, and special spatial structure deserve comment and will be the focus of much future research. In Sec. V we will present numerical results which indicate that compact support, not necessarily positive initial conditions, converge to the preferred front through the continuum of oscillatory fronts. Convergence of front speeds is shown to be from below the final front speed, which is consistent with the idea that the transient oscillatory fronts organize the convergence of fronts. Comparisons of the spatial structures of the evolving initial conditions and ODE front solutions with the same speed support our contention that the manifold of oscillatory fronts is a preferred manifold along which solutions evolve. When the fronts converge to the WTC solution, they may leave behind a wave singularity. This wave singularity is a superposition of a stationary solution connecting positive and negative finite amplitude states and a front moving with the asymptotic nonlinear velocity. It is also the residue of the transient oscillatory states, as we will also discuss in Sec. V. In Sec. VI we will use a Liapunov functional to illustrate why oscillatory fronts appear as transients and also why nonoscillatory fronts are inaccessible from compactly supported, nonpositive definite initial conditions. Finally, in Sec. VII we will compare and contrast our results with those of van Saarloos, who produced many of these results about asymptotic states in a different context.

II. THE KOLMOGOROV-LANGER APPROACH

Consider the PDE

$$u_t=\mu u+u_{xx}+u^3-u^5 . \tag{8}$$

A front solution to (6) is a solution $u(x,t)=u(x-ct)$, which satisfies the boundary conditions

$$u\to 0$$

as $x\to\infty$,

$$u\to u_s$$

as $x\to-\infty$, and

$$u_s^4-u_s^2-\mu=0 .$$

When $\mu>0$ the solution $u=0$ is unstable and there is only one positive root for u_s.

A traditional method for determining the asymptotic speed of a front from general initial conditions is the Kolmogorov stationary-phase argument and method of steepest descent. We propose a broadband initial condition for (6),

$$u(x,0)=u_i(x) ,$$

with

$$\int_{-\infty}^{\infty}|u_i|dx\ll 1 .$$

Given an initially localized disturbance about the unstable state, we ask how the disturbance spreads and propagates. Since the stable finite-amplitude state has size of order 1, it is only the initial condition that must be restricted in size. This allows us to restrict ourselves to the linear part of the equation, and we may write

$$u(x,t)=\int_{-\infty}^{\infty}\hat{u}(k)\exp[ikx+\Omega(k)t]dk\ , \tag{9}$$

where

$$\hat{u}(k)=\frac{1}{2\pi}\int_{-\infty}^{\infty}u_i(x)\exp(-ikx)dx$$

and

$$\Omega(k)=\mu-k^2\ .$$

The form of $\Omega(k)$ follows from the linear portion of (6).

To determine the preferred front speed we will evaluate (9) asymptotically for large t in the region

$$x=z+ct$$

with z and c both of order 1, c undetermined. In terms of z and c (9) becomes

$$u(z,t)=\int_{-\infty}^{\infty}\hat{u}(k)\exp[ikz+h(k)t]dk\ , \tag{10}$$

with

$$h(k)=ick+\Omega(k)\ .$$

We will evaluate (10) using the method of steepest descent. Asking that $h(k)$ be maximal provides the requirement

$$h'(k)=0\ ,$$

or

$$ic+\Omega'(k)=ic-2k=0\ ,$$

$$c^*=-2ik^*\ .$$

Here the asterisk denotes a quantity determined via steepest descent. Hence

$$h(k^*)=\mu+(k^*)^2\ .$$

For this approximation to be stable in time an additional requirement must be satisfied;

$$\mathrm{Re}[h(k^*)]=0\ , \tag{11}$$

which is the requirement that we choose a speed at which the phase is stationary. The asymptotic form for u is given

$$u(z,t)=\hat{u}(0)e^{\lambda^* z}\int_{-\infty}^{\infty}\exp[\tfrac{1}{2}h''(0)k^2t]dk\ ,$$

with $c^*=2\sqrt{\mu}$ and $\lambda^*=-\sqrt{\mu}$. Since $h''(0)=-2$ we get

$$u(z,t)=\hat{u}(0)e^{\lambda^* z}\left[\frac{\pi}{t}\right]^{1/2}\ . \tag{12}$$

As we will show later, the asymptotic front speed c^* is the maximum speed in the continuum of possible front speeds.

Using the method of stationary phase on either Eq. (3) or (7) is no more difficult. In the case of (3), $c^*=2$ regardless of the parameter b, and $\lambda^*=-1$. In the case of (7), the asymptotic form of the marginal front is given by

$$A(z,t)\sim e^{(\lambda^*+ik^*)z+i\omega^*t}\left[\frac{\pi}{(1+i\beta)t}\right]^{1/2}\ .$$

The speed of this marginal solution is the same as the real version,

$$c^*=2\sqrt{\mu}\ ,$$

with

$$k^*=\frac{\beta\sqrt{\mu}}{(1+\beta^2)^{1/2}},\quad \lambda^*=-\frac{k^*}{\beta},\quad \omega^*=c^*k^*-\beta\mu\ .$$

III. AN INTEGRABLE FRONT FROM THE WTC METHOD

Even though c^* is the maximal speed in the continuum of front speeds, it is possible for a front to have a speed $\tilde{c}$ with $\tilde{c}\geq c^*$. When $\mu<0$, fronts are possible (see Jones, Kapitula, and Powell [15]), even though the linear marginal speed c^* does not exist. When $\mu>0$ and small, c^* is also small and the branch of fronts from the first-order transition may have greater speed than the Kolmogorov speed. A closed-form solution for such a front may be found using the WTC method, as discussed in Cariello and Tabor [14].

We begin the WTC method by finding a leading balance for (6). Let

$$u(x,t)=\phi(x,t)[\alpha(x,t)]^{\epsilon}\ .$$

The function α is the singular manifold and the scalar ϵ a (negative) power yet to be determined. As $\alpha\to 0$, we expect the highest-order derivatives in (6) to balance the biggest nonlinearities. Therefore to leading order in α,

$$\phi\alpha^{\epsilon-2}\alpha_x^2=u_{xx}\sim u^5=\phi^5\alpha^{5\epsilon}\ .$$

The relation $5\epsilon=\epsilon-2$ determines

$$\epsilon=-\tfrac{1}{2}\ .$$

We seek a truncated Painlevé expansion

$$u=\phi(x,t)\alpha(x,t)^{-1/2}\ . \tag{13}$$

Equation (6) becomes

$$\phi_t\alpha-\tfrac{1}{2}\phi\alpha_t=\mu\phi\alpha+\phi_{xx}\alpha-\phi_x\alpha_x -\tfrac{1}{2}\phi\alpha_{xx}+\tfrac{3}{4}\phi\alpha_x^2\alpha^{-1}+\phi^3-\phi^5\alpha^{-1}\ .$$

Collecting similar powers of α gives an overdetermined system of equations for ϕ and α:

$$\phi^4=\tfrac{3}{4}\alpha_x^2\ , \tag{14}$$

$$\alpha_t=2\frac{\phi_x}{\phi}\alpha_x+\alpha_{xx}-2\phi^2\ , \tag{15}$$

$$\phi_t=\mu\phi+\phi_{xx}\ . \tag{16}$$

From $\phi^2=\pm(\sqrt{3}/2)\alpha_x$, $2\phi\phi_x=\pm(\sqrt{3}/2)\alpha_{xx}$, and dividing gives

$$2\frac{\phi_x}{\phi}=\frac{\alpha_{xx}}{\alpha_x} .$$

Equation (15) becomes

$$\alpha_t=2\alpha_{xx}\mp\sqrt{3}\alpha_x . \tag{17}$$

Deriving (17) with respect to x and using various derivatives of (14) yields

$$\phi_t=2\frac{\phi_x^2}{\phi}+2\phi_{xx}\mp\sqrt{3}\phi_x . \tag{18}$$

Equating ϕ_t in (16) and (18) gives an equation for the spatial dependence of ϕ,

$$\phi_{xx}\mp\sqrt{3}\phi_x+2\frac{\phi_x^2}{\phi}-\mu\phi=0 . \tag{19}$$

Equation (19) has solutions $\phi\sim\exp(\lambda x)$ with

$$\lambda=\frac{\sqrt{3}}{6}[\pm1+(\pm)\sqrt{1+4\mu}] . \tag{20}$$

Equation (16) gives the time dependence for ϕ,

$$\phi_t=(\mu+\lambda^2)\phi ,$$

and hence

$$\phi=\phi_0\exp\left[\lambda\left[x+\frac{\mu+\lambda^2}{\lambda}t\right]\right] .$$

We require $\phi\to0$ as $x\to\infty$ for a front solution. Therefore $\lambda<0$. To determine α,

$$\alpha_x=\pm\frac{2}{\sqrt{3}}\phi^2=\pm\frac{2}{\sqrt{3}}\phi_0^2e^{2\lambda[x+(\mu+\lambda^2/\lambda)t]} ,$$

so that

$$\alpha=\pm\frac{\phi_0^2}{\lambda\sqrt{3}}(1+e^{2\lambda[x+(\mu+\lambda^2/\lambda)t]}) .$$

Here we have used translational invariance to conveniently determine the arbitrary constant.

Since α appears as a square root in u, we must choose the minus sign above [both minus signs in (20)]. This gives a solution for u

$$u=\frac{-\frac{\sqrt{3}\tilde{\lambda}}{\phi_0}e^{\tilde{\lambda}z}}{(1+e^{2\tilde{\lambda}z})^{1/2}} ,$$

with

$$\begin{aligned} &z=x-\tilde{c}t , \\ &\tilde{c}=-\frac{\mu+\tilde{\lambda}^2}{\tilde{\lambda}},\quad \tilde{\lambda}=-\frac{\sqrt{3}}{6}(1+\sqrt{1+4\mu}) . \end{aligned} \tag{21}$$

With the boundary equation $u\to u_s$ as $x\to-\infty$, we can determine ϕ_0 and the final form of the WTC solution

$$u=\frac{u_se^{\tilde{\lambda}z}}{(1+e^{2\tilde{\lambda}z})^{1/2}} . \tag{22}$$

The above special solution using the WTC method is equivalent to the nonlinear solution found by van Saarloos. In fact, if the overdetermined system of equations arising from the WTC approach is written in a traveling frame, one is directly led to van Saarloos's reduction of order. van Saarloos supposed that the special solution satisfies a first-order ODE in the traveling frame of reference,

$$u_z=h(u)=au+bu^3 , \tag{23}$$

with a, b, and the front speed c undetermined. The constants are determined by requiring that (23) also satisfy (6) written in a traveling frame of reference,

$$u_{zz}+cu_z+\mu u+u^3-u^5=0 . \tag{24}$$

Substituting (23) into (24) and equating powers of u gives an algebraic system which may be solved for a, b, and c. In terms of quantities we have determined, the solution is

$$a=\tilde{\lambda},\quad b=\frac{1}{\sqrt{3}},\quad c=\tilde{c} .$$

This immediately gives the solution (22).

To show that (23) is equivalent to the system (14)–(16), let us begin by substituting the form (13) into (23). This gives two equations at different orders in α,

$$\phi_z=a\phi \tag{25}$$

and

$$-\alpha_z=2b\phi^2 . \tag{26}$$

Comparing (26) with (14) makes it clear that $b=1/\sqrt{3}$, which is what van Saarloos determined. On the other hand, deriving (25) with respect to z and adding $\mu\phi$ to both sides gives

$$\phi_{zz}+\mu\phi=a\phi_z+\mu\phi=\left[\frac{a^2+\mu}{a}\right]\phi_z ,$$

which is equivalent to (16) written in a traveling frame with speed

$$-c=\frac{a^2+\mu}{a}=\frac{\tilde{\lambda}^2+\mu}{\tilde{\lambda}}=-\tilde{c}$$

as determined above. Finally, if we substitute (25) into the last determining equation of the WTC method, (18), we get an algebraic condition on a,

$$3a^2+\sqrt{3}a-\mu=0 .$$

However, this is precisely the same as $a=\tilde{\lambda}$ above. Thus, using the WTC method to find an integrable trajectory gives rise naturally to van Saarloos's ansatz that the nonlinear trajectory may be written as the solution to a first-order ODE.

Recall now that the linear marginal speed found in Sec. II, c^*, is supposed to be the maximal possible speed. Now we will show that it is possible for $\tilde{c}>c^*$ and $\tilde{\lambda}<\lambda^*$ in some parameter regimes. The asymptotic form of a front approaching zero is $e^{\lambda z}$, with $\lambda<0$. Therefore, when $\tilde{c}>c^*$ and $\tilde{\lambda}<\lambda^*$ the nonlinear front is more rapid than the linear, and has a steeper decrease to the zero

state. In a stationary frame of reference, this corresponds to a more rapid departure from the unstable zero state, which we will discuss more precisely in Secs. IV and V. The range of μ for which this happens is defined by

$$-\frac{\mu+\tilde{\lambda}^2}{\tilde{\lambda}}=\tilde{c}>c^*=2\sqrt{\mu} \tag{27}$$

or

$$32\mu^2+10\mu+1+(8\mu+1)\sqrt{1+4\mu}>24\mu(1+2\mu+\sqrt{1+4\mu})$$

after squaring both sides. Note that (27) is certainly satisfied for μ either small or negative. Simplifying (27),

$$2\mu(4\mu-1)+(1-4\mu)\sqrt{1+4\mu}>-1$$

or

$$0>(1-4\mu)\sqrt{1+4\mu}>-1-2\mu(4\mu-1)\ .$$

The first inequality comes from assuming $4\mu-1>0$, since we know (27) holds for μ small. Squaring gives

$$(1+4\mu)(1-4\mu)^2<1+4\mu(4\mu-1)+4\mu^2(4\mu-1)^2$$

and simplifying

$$\mu-\tfrac{3}{4}<0\ .$$

Therefore, for $\mu<\mu_c=\frac{3}{4}$ we have $\tilde{c}>c^*$.

The parameter regime for which $\tilde{\lambda}<\lambda^*$ is the same. We want μ such that

$$-\frac{\sqrt{3}}{6}[1+\sqrt{1+4\mu}]=\tilde{\lambda}<\lambda^*=-\sqrt{\mu}\ .$$

Squaring and simplifying yields

$$\sqrt{1+4\mu}>4\mu-1\ ,$$

and squaring again yields (with simplification)

$$3>4\mu\ .$$

Thus we may write $\tilde{c}>c^*$ and $\tilde{\lambda}<\lambda^*$ when $\mu<\mu_c=\frac{3}{4}$.

When the WTC method is applied to (3), the resulting front solution has the form

$$u=\frac{e^{\tilde{\lambda}(x-\tilde{c}t)}}{e^{\tilde{\lambda}(x-\tilde{c}t)}+1}\ ,$$

and the parameters are determined as functions of b. By comparing the asymptotic steepness of this special solution with the marginal solution, we find $\tilde{c}>c^*$ and $\tilde{\lambda}<\lambda^*$ when either $b<\frac{1}{2}$ or $b>2$. In the former case

$$\tilde{c}=\sqrt{2b}+\frac{1}{\sqrt{2b}},\quad \tilde{\lambda}=-\frac{1}{2\sqrt{b}}\ .$$

In the latter case

$$\tilde{c}=\frac{\sqrt{2}}{\sqrt{b}}+\frac{\sqrt{b}}{\sqrt{2}},\quad \tilde{\lambda}=-\frac{\sqrt{b}}{\sqrt{2}}\ .$$

When the WTC method is applied to (7), the leading-order term is complex. The method yields a system of six overdetermined equation analogous to those described by Cariello and Tabor for (2). In this case, the solution is

$$A(x,t)=\mathrm{Re}^{i\eta x+i\nu t}\frac{\sqrt{\exp[2\tilde{\lambda}(x-\tilde{c}t)]}}{\{1+\exp[2\tilde{\lambda}(x-\tilde{c}t)]\}^{1/2+bi}}\ .$$

The parameters in this solution are given by choosing $\pm$ based on $\beta\lesseqgtr 0$,

$$b=\frac{2\pm(4+\beta^2)^{1/2}}{2\beta}\ ,$$

$$K=(\tfrac{3}{4}-2\beta b-b^2)^{1/2}\ ,$$

$$\tilde{\lambda}^2\left[12+\left[4\beta-K\frac{\gamma-2b}{1+4b^2}\right]^2\right]-4K\tilde{\lambda}\frac{1+2b\gamma}{1+4b^2}-4\mu=0\ ,$$

$$R^2=K\tilde{\lambda}\ ,$$

$$\tilde{c}=\frac{K(1+\beta\gamma+2b\gamma-2b\beta)}{1+4b^2}-4\tilde{\lambda}(1+\beta^2)\ ,$$

$$(\eta-2b\tilde{\lambda})^2=\mu+K\tilde{\lambda}^2-K^2\tilde{\lambda}^4\ ,$$

and finally

$$\nu=2b\tilde{c}\tilde{\lambda}+\gamma R^2-\beta(\eta-2b\tilde{\lambda})^2\ .$$

This solution predominates when $-\lambda^*<-\tilde{\lambda}$.

Although these solutions and their regime of dominance appear complicated, the analysis is the same in character. In a well-defined range of parameter space, the envelope of the WTC solution has steeper descent and more rapid speed than the linear solutions resulting from the stationary-phase analysis. In Sec. IV we will discuss how the special front solution with speed $\tilde{c}$ relates to the continuum of possible front solutions with maximum speed c^*.

IV. ACCESSIBLE FRONT SPEEDS

The purpose of this section is to determine a class of accessible front solutions in connection with (6). First we will examine the structure of solutions to (6) in a traveling frame of reference. Next we will suggest that some of these solutions are inadmissible because they are not approached from compact support initial conditions. Finally, we will show that the class of allowable (in the above sense) transient front speeds is the continuum $[0,c^*]$, together with the unique front speed $\tilde{c}$.

Any front solution to (6) moving with speed c must satisfy (24), the ODE

$$u_{zz}+cu_z+\mu u+u^3-u^5=0\ ,$$

with $z=x-ct$. As $z\to-\infty$, $u\to u_s$ with u_s the positive root of

$$f(u)=\mu u+u^3-u^5\ .$$

The trajectories in the ODE corresponding to fronts can readily be understood as the dynamics of a damped oscillator. Multiplying (24) by u_z and regrouping gives

$$-cu_z^2=\frac{d}{dz}E(u)\ , \tag{28}$$

where

$$E(u)=\tfrac{1}{2}u_z^2+V(u) \tag{29}$$

and

$$V(u)=\frac{\mu}{2}u^2+\tfrac{1}{4}u^4-\tfrac{1}{6}u^6 . \tag{30}$$

$E(u)$ is the total energy at some point z in the trajectory u, $V(u)$ is the potential energy, and (28) is a statement of conservation of total energy (or lack thereof). The function $V(u)$ is graphed for $\mu>0$ and $\mu<0$ in Figs. 1(a) and 1(b), respectively. The left-hand side of (28) is a damping or friction term with damping coefficient c. A front solution is a trajectory connecting potential energy extrema at $u=u_s$ and $u=0$. When $\mu<0$ the two extrema are maxima and a unique damping value must be chosen for the trajectory to start and end at the right place. When $\mu>0$, zero is in a potential well and it is possible to make a front connection for any $c>0$. When $c<2\sqrt{\mu}$, the solution oscillates about zero. Critical damping occurs for $c=c^*=2\sqrt{\mu}$, and larger values of c give overdamped solutions.

Note that when $\mu<0$ the only front connection possible is the WTC front. Zero is a potential maximum, and therefore (as can be seen below) it is a saddle point for $\mu<0$. Hence, when the unstable manifold of u_s intersects the stable manifold of zero, it is tangential to the strongly attracting eigendirection (in this case it is the only attracting eigendirection). Thus supercritical WTC fronts that occur when $\mu<\mu_c$, the regime in which the WTC solutions are predominant, are a continuous deformation

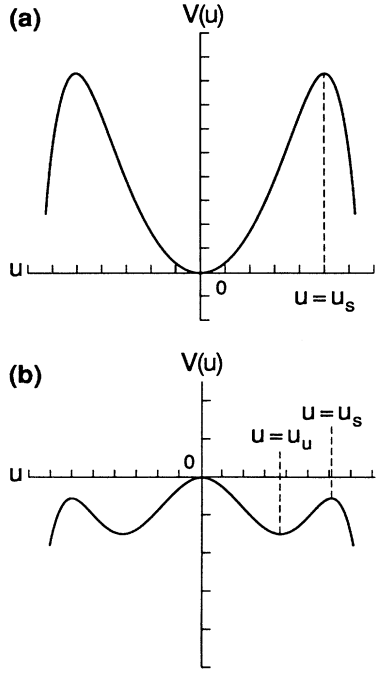

FIG. 1. (a) Potential $V(u)$ in the supercritical $\mu>0$ case. (b) Potential $V(u)$ in the subcritical $\mu<0$ case.

of the subcritical front solutions. As μ is increased past the critical value, these solutions do not vanish. Instead they attach to the *weakly* attracting manifold of zero, and hence do not satisfy either $\tilde{c}>c^*$ or $\lambda^*>\tilde{\lambda}$.

Let $u=u_s+\hat{u}$, and linearize (24); the linear behavior of a front at $-\infty$ is governed by

$$\hat{u}_{zz}+c\hat{u}_z+\hat{u}f'(u_s)=0 .$$

The corresponding characteristic polynomial

$$\eta^2+c\eta+f'(u_s)=0$$

has roots

$$\eta=-\frac{c}{2}\pm\left[\frac{c^2}{4}-f'(u_s)\right]^{1/2} .$$

Since $f'(u_s)<0$ one root is positive and the other negative for any front speed c. Thus u_s is always a saddle point for (24), and a front solution follows the unstable manifold of u_s.

On the other hand, as $z\to\infty$, $u\to 0$ and the linear behavior of a front solution is governed by the equation

$$u_{zz}+cu_z+\mu=0 .$$

The corresponding characteristic equation is

$$\lambda^2+c\lambda+\mu=0 , \tag{31}$$

with roots

$$\lambda=-\frac{c}{2}\pm\left[\frac{c^2}{4}\right]^{1/2}-\mu .$$

Both roots are negative for $\mu>0$, so a front solution following the unstable manifold of u_s is always attracted to zero. Generically, a front trajectory will approach zero tangential to the *weaker* of the two eigendirections. Thus we may write the asymptotic exponential dependence of a front solution to (24) as

$$\lambda_{\mathrm{ODE}}(c)=\mathrm{Re}\left[-\frac{c}{2}+\left[\frac{c^2}{4}\right]^{1/2}-\mu\right] .$$

The real part has been taken so that when $c^2<4\mu$, λ_{ODE} will give the asymptotic decrease of the envelope of the oscillation.

Already a contradiction seems unavoidable. We have a closed-form front solution with speed $\tilde{c}$ from the WTC analysis and asymptotic exponential dependence

$$\tilde{\lambda}=-\frac{\tilde{c}}{2}-\left[\frac{\tilde{c}^2}{4}\right]^{1/2}-\mu .$$

Clearly $\tilde{\lambda}\neq\lambda_{\mathrm{ODE}}(\tilde{c})$, except when $\tilde{c}=2\sqrt{\mu}$. This contradiction can be resolved by realizing that (24) allows a nongeneric connection between u_s and zero along the strongly stable eigendirection of zero. We will call such a connection *strongly heteroclinic* (SH). A strongly heteroclinic connection occurs when the unstable manifold of u_s intersects the strongly attracting eigendirection of zero tangentially.

When a SH connection is *not* possible, the phase space

of (24) varies with c at a particular value of $\mu > \mu_c$ according to Figs. 2(a)–2(c). When a SH connection does exist, the variation of the phase space with c is more complicated, as depicted in Figs. 3(a)–(e). Since $\tilde{\lambda}$ satisfies (31) with speed $\tilde{c}$, but $\tilde{\lambda} \neq \lambda_{\mathrm{ODE}}(\tilde{c})$, the special WTC solution (22) is the nongeneric SH connection depicted in Fig. 3(b).

The front solutions we are interested in must satisfy not only (24) but be accessible to the PDE (6) from compact support initial conditions as well. Essentially, this means that as a front solution develops from some perturbation about zero, it must grow along the most temporally unstable mode available to it. Our ansatz is that if this most unstable mode is the asymptotic behavior of a front ODE solution, then that front is accessible. Let $u(x-ct)$ be a front solution to (24) with asymptotic dependence as $u \to 0$

$$u(z) \sim u^{+}(c) e^{\lambda^{+} z} + u^{-}(c) e^{\lambda^{-} z} ,$$

where $\lambda^{\pm}$ are the greater and lesser roots of (31) [i.e., $\mathrm{Re}(\lambda^{+}) = \lambda_{\mathrm{ODE}}(c)$]. The constants $u^{\pm}$ depend on which front solution we have. At a particular location x_0 in x the PDE gives

$$u(x_0,t) \sim u^{+}(c) e^{\lambda^{+} x_0} e^{\sigma^{+} t} + u^{-}(c) e^{\lambda^{-} x_0} e^{\sigma^{-} t} ,$$

where $\sigma^{\pm} = -c\lambda^{\pm}$. When $\sigma^{-} > \sigma^{+}$, which occurs when $c > c^{*}$, the mode $\exp(\lambda^{-} z)$ grows exponentially faster at a point x_0. A random perturbation from zero follows the most unstable mode $\exp(\lambda^{-} z)$. Thus the PDE determines that accessible fronts have asymptotic dependence

$$\lambda_{\mathrm{PDE}}(c) = \mathrm{Re}(\lambda^{-}) = \mathrm{Re}\left[-\frac{c}{2} - \left[\frac{c^2}{4} - \mu \right]^{1/2} \right] .$$

When $\lambda_{\mathrm{ODE}} c \neq \lambda_{\mathrm{PDE}}(c)$ the asymptotic behaviors dictated by (6) and (24) are not compatible. Therefore approachable front solutions cannot exist when $\lambda_{\mathrm{ODE}}(c) \neq \lambda_{\mathrm{PDE}}(c)$. When $c^2 < 4\mu$, $\lambda_{\mathrm{ODE}}(c) = \lambda_{\mathrm{PDE}}(c)$, and this defines a continuum of allowed front speeds. The exception is the SH front speed $\tilde{c}$, and since $\tilde{\lambda} = \lambda_{\mathrm{PDE}}(\tilde{c})$, the set of allowable front speeds is $[0, 2\sqrt{\mu}] \cup \{\tilde{c}\}$. From this point of view, we should expect that the asymptotic front speed which emerges from compact support initial conditions should be that front giving maximum temporal growth rate about the unstable state. This growth rate satisfies

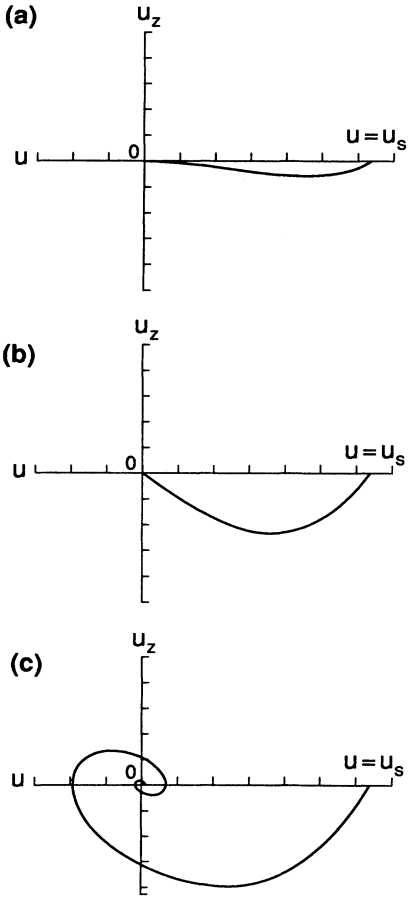

FIG. 2. (a) Overdamped front in phase space $c > c^{*}$ and no SH connection possible. (b) Marginal front in phase space $c = c^{*}$ and no SH connection possible. (c) Oscillatory front in phase space $c < c^{*}$ and no SH connection possible.

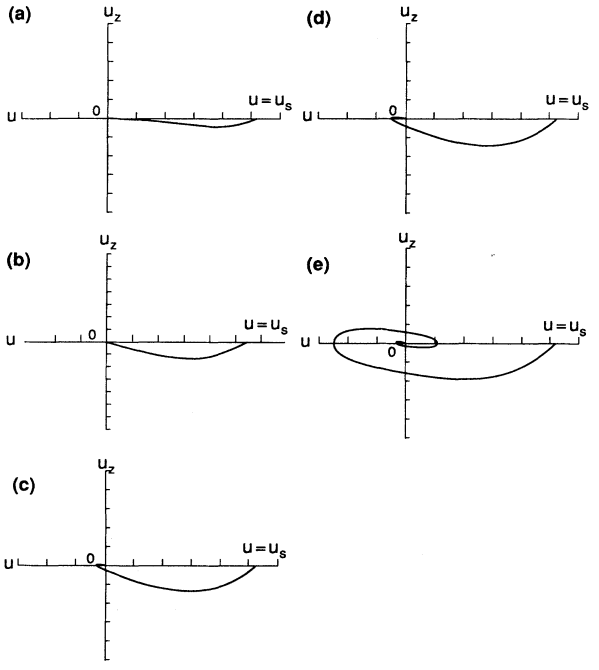

FIG. 3. (a) Overdamped front in phase space $c > \tilde{c}$ and SH connection possible. (b) Strongly heteroclinic WTC front $c = \tilde{c}$. (c) Overdamped solutions approaching zero from negative side of phase space $\tilde{c} > c > c^{*}$. (d) Marginal front in phase space $c = c^{*}$ and the SH connection is possible. Solution approaches zero from negative side of phase space. (e) Oscillatory front in phase space $c < c^{*}$ and SH connection is possible.

$$\sigma = -c\lambda_{\mathrm{PDE}} = \frac{c^2}{4}$$

when $c \le c^*$. Thus c^* is the speed corresponding to maximum growth rate for a front with speed in the continuum of accessible speeds. When $\tilde{c} > c^*$, $\tilde{\lambda} < \lambda^*$ and the SH front speed will have the greater pointwise growth rate in time. We will demonstrate numerically in Sec. V that truncated fronts in the real equation always converges to the accessible front with maximum speed, either c^* or $\tilde{c}$. This is equivalent to steepest envelope in the real equation, and we will show that van Saarloos's steepest envelope criterion is equivalent to maximum temporal growth about zero. Similar results apply to fronts in Eqs. (3) and (7), where c^* and $\tilde{c}$ are determined as in Sec. II and III.

V. CONVERGENCE OF FRONTS

Our idea is that the continuum of speeds below c^* is the dynamically relevant set of speeds. The stable $c > c^*$ (except for $\tilde{c}$) fronts are inaccessible from compact support initial conditions. The oscillatory fronts are unstable, but they are "observable" because in the presence of oscillatory perturbations they exist as transients. These transients vanish only algebraically rapidly and serve to organize the convergence of speeds to either c^* or $\tilde{c}$. We now illustrate this picture with numerical evidence. The continuum of front speeds and the accompanying trajectories of (24) seem to define an attracting manifold for the PDE (6). If we start with an initial condition on this manifold, we expect the speed of the solution to evolve to either c^* or $\tilde{c}$ by accelerating along this manifold. We might also expect the convergence to be algebraic, since the entire continuum satisfies the PDE. On the other hand, from initial conditions given by (truncated) solutions to (24) with $c > c^*$, we will show that solutions collapse to the attracting continuum of fronts and then evolve along it. Of course, this can only happen if we allow nonpositivity in the initial condition, for instance, possibly negative infinitesimal perturbations about zero. When we extend this work to complex equations like (2) or (7), which may be derived in many physical contexts, positivity has no meaning. Consequently, in the present work we will not enforce positivity or rely upon it, but rather allow random fluctuations of any sign about the unstable zero state. How the solutions make the jump from the continuum to the SH front when there is a separation between the two is a question yet to be resolved. The numerical results will answer this question, as well as verify convergence along the continuum of fronts (with a caveat).

Solutions to the full PDE were obtained using a split-step, Fourier differencing in space, with a Runge-Kutta time method. The accuracy of this method in these kinds of problems is documented (see, for example, Bernoff [16]). Solutions to the ODE, which we used as initial conditions, were obtained by using a Runge-Kutta method to trace the unstable manifold of the finite amplitude state u_s. Our basic methodology is to initialize the PDE with truncated ODE front solutions of a particular speed c_0. Since the domain is periodic, we reflect the ODE solution about zero so that the initial condition becomes a lump. The right and left sides of this lump look like fronts propagating with speed $\pm c_0$.

Figure 4 is a series of time slices taken of a solution for $\mu = 0.81$. The initial condition is a reflected front solution to the ODE with speed $c_0 = 1.5$. In this regime, $\tilde{c} < c^* = 1.8$, so that the initial condition is an oscillatory front. At each slice in time we diagnose a front speed by taking

$$c_{\mathrm{local}} = \left. \frac{u_t}{u_x} \right|_{u = u_0}$$

from the PDE. This ratio is evaluated at the first place where the solution u reaches the value u_0 (in our simulations $u_0 = 0.05$). For each time slice we plotted the solution in the phase space (u, u_z), and the results are the solid curves in Fig. 4. The dashed curve in the same phase space are ODE solutions to (24) with speed c_{local} diagnosed as above. It is clear from Fig. 4 that the solution converges to the maximum speed solution along the manifold of front solutions. Figure 5 is a plot of the local speeds (solid) starting at time zero and ending at time 15. Note that in Fig. 5 the convergence of front speeds is from below c^*. The dashed curve in Fig. 5 is a plot of

$$v(t) = c^* - \frac{c^* - c_0}{1+t}\ , \tag{32}$$

which we have included to illustrate that the convergence of speeds is algebraic through the continuum of fronts. As we will discuss in Sec. VI, the local speeds should converge to c^* more rapidly than (32), which is borne out by Fig. 5.

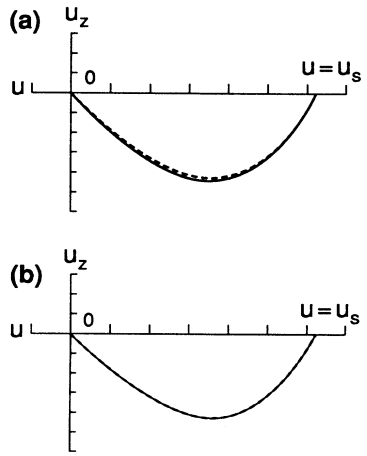

FIG. 4. (a) Solution at time 3.0, $\mu = 0.81$, and $c_0 = 1.5$. The solid curve is the solution, while the dashed curve is the ODE approximation using diagnosed local speed. (b) Solution at time 15.0, $\mu 0.81$, and $c_0 = 1.5$. The solid curve is the solution, while the dashed curve is the ODE approximation using diagnosed local speed.

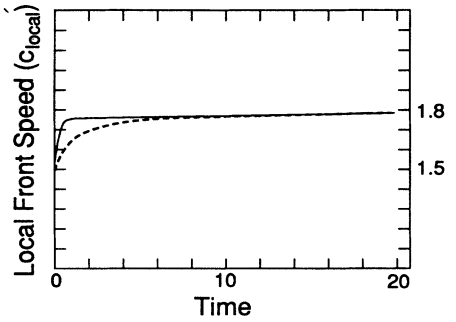

FIG. 5. Local front speeds for $\mu=0.81$, and $c_0=1.5$. The solid curve is the local front speed diagnosed in the tail, while the dashed curve is proportional to 1/(time) and converges to $c^*=1.8$. Note that convergence is from below the marginal speed.

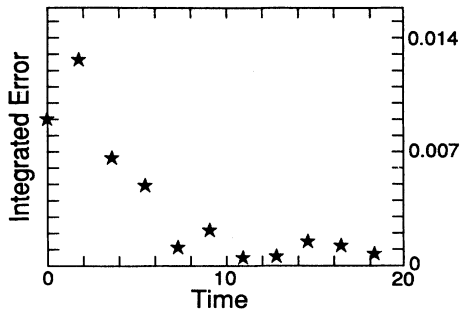

FIG. 6. Distance between transients and the manifold of front solutions according to the norm D. The initial condition is oscillatory and on the manifold of fronts with speed $c_0=1.5$ for $\mu=0.81$. As predicted the distance is very close to zero, indicating that oscillating fronts accelerate along the manifold of fronts to their asymptotic state.

A major point we are making, which requires additional support, is that the solutions are actually close to the manifold of oscillating fronts as they develop toward the asymptotic state. Let

$$U(x)=u(x-c_{\text{local}}t_0)$$

be the ODE solutions obtained to (24) with speed c_{local} diagnosed as above. We define the distance norm $D(U,u)$ as

$$D(U,u)=\min_{x_0}\int |U(x-x_0)-u(x,t_0)|dx\ ,$$

where $U(x,t_0)$ is the transient PDE solutions, obtained numerically and "frozen" in time at $t=t_0$. The minimization is included to take into account the translational invariance of solutions; practically, this is equivalent to choosing x_0 so that

$$u(x_0,t_0)=U(0)\ .$$

S Lince $D(U,u)$ must be obtained numerically, and x_0 may fall between grid points, the numerical approximation to D is accurate to within a factor proportional to δx. In these runs the number of points was 1024 on half an interval of length 40π, giving an accuracy of order 10^{-2}.

Figure 6 is a plot of the integrated error $D(U,u)$ at several slices in time. Note that the integrated error is as close to zero as can be expected with the accuracy of this numerical approximation. This conclusively demonstrates that slower fronts develop toward their asymptotic state by accelerating along the manifold of oscillatory fronts.

Figure 7 is a plot of local speeds for a solution with initial condition having speed $c_0=2.5$ and $\mu=0.81$. Note that the local speed collapses rapidly to a speed $c_{\text{local}}<c^*$ and then begins to approach the final speed. An exact solution with speed 2.5 would presumably be stable, but clearly the approximate solution from ODE shooting, truncated in its tail, is not. This indicates that the continuum of fronts with $c<c^*$ is in some sense attracting, while the $c>c^*$ front are not. Figure 8 is a plot of several time slices of the solution, beginning with the overdamped initial condition, graphed in space.

In the earlier plot of the error norm, positivity was violated by the initial condition since we started with an oscillatory front. In the current case, however, the initial condition was non-negative. Positivity was violated by small numerical perturbations about zero, corresponding to unstable modes in the PDE. We allowed this sort of perturbation in keeping with our desire to produce results that would extend to complex equations. Figure 9 is a plot of the integrated error D for several different times. Initially, the error is very small because we start with a monotone front solution. As this collapses toward the manifold of oscillating fronts the error grows large, and as it moves along the manifold the error is uniformly small. This supports our contention that the $c<c^*$ fronts are dynamically relevant and attracting in the presence of oscillating perturbations.

In the previous two examples, the maximum allowable

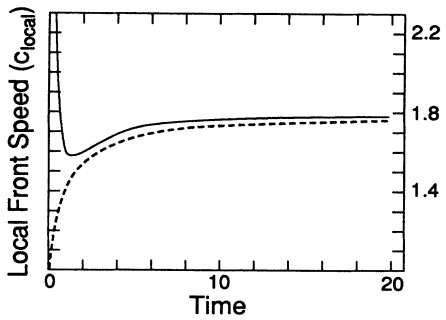

FIG. 7. Local front speeds for $\mu=0.81$ and $c_0=2.5$. The curve labeled A is local front speed diagnosed in the tail, while the curve labeled B is proportional to 1/(time) and converges to $c^*=1.8$. Note that the higher speeds collapse rapidly to the continuum of speeds and then converge from below.

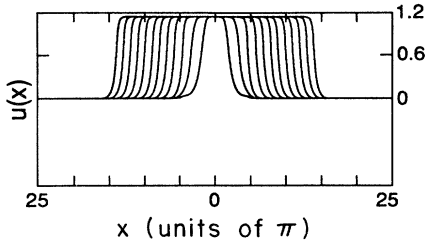

FIG. 8. Time slices of the solution with $\mu=0.81$ and $c_0=2.5$ plotted as functions of space. Time slices are 1.33 units apart in time.

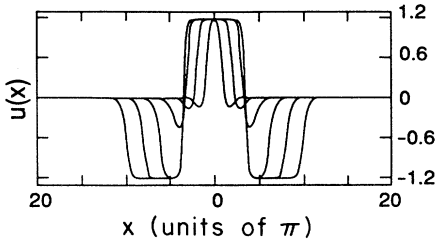

FIG. 10. Time slices of the solution with $\mu=0.64$ and $c_0=1.0$ plotted as functions of space. Time slices are 1.33 units apart in time. Note that the asymptotic form of the front converges from the negative side and leaves behind an essentially motionless singularity.

front speed c^* is a member of the continuum of stable speeds. In the next example, $\mu=0.64<\mu_c=0.75$. As discussed in Sec. III, the maximum speed in this regime is $\bar{c}$, the SH front speed, which is separate from the continuum. A front initialized in the continuum must somehow make the jump from the end of the continuum c^* to the final speed $\bar{c}$.

Figure 10 is analogous to Fig. 8, with $\mu=0.64$ and $c_0=1$. Figure 11 is a plot of local front speeds (solid) compared with (32) (dashed). Note that while the tail of the front converges to the appropriate form and speed, it does so from the *negative* side and leaves behind an essentially motionless connection between $\pm u_s$, the positive and negative stationary states. If we momentarily view u as the amplitude of a complex function, this motionless connection between $\pm u_s$ occasions a jump of π in the wave number, and the fronts are therefore converging by leaving behind a wave singularity.

The unique convergence is forced by competition between the attracting front manifold and the spatial dominance of the SH solution in the ODE phase space. An initially oscillatory front at time zero looks like Fig. 3(e). As it accelerates along the manifold of fronts, its oscillation about zero slowly unwinds. As the local speed of the solution approaches c^*, the shape of the front approaches the front in Fig. 3(d). Since μ is small in this regime, at the marginal speed the attraction of the origin is not powerful enough to keep the solution from overshooting zero. Once it has overshot, it must be attracted to zero along the degenerate eigendirection from the *negative* side, as depicted in Fig. 3(d).

At this point in its convergence the solution is faced with trouble. The temporal dynamics of the tail push it to converge to the SH solution, but staying near the manifold of fronts traps it on the negative side of the strongly attracting eigendirection. The strongly stable manifold, which is a continuous deformation of the degenerate eigendirection at c^*, pushes the solution to the weakly stable manifold on the negative side of the phase space. This prohibits the solution from converging to the strongly stable manifold in the vicinity of zero. To connect to the strongly stable manifold on the negative side,

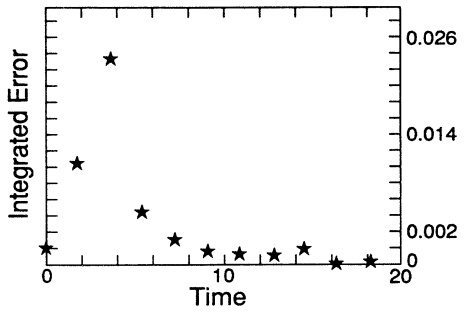

FIG. 9. Distance between transients and the manifold of front solutions according to the norm D. The initial condition is strictly positive and on the manifold of fronts with speed $c_0=2.5$ for $\mu=0.81$. The initial distance is very small because we begin with a front solution. As the solution collapses toward the manifold of oscillating fronts, the distance is large. Once the manifold is reached, however, the distance between the transient and the corresponding front is uniformly small, which indicates that the manifold of oscillating fronts is attractive and organizes the convergence of front solutions.

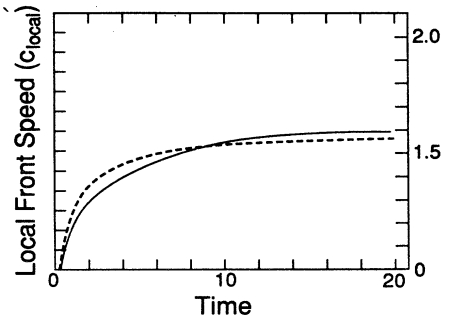

FIG. 11. Local front speeds for $\mu=0.64$ and $c_0=1.0$. The solid curve is local front speed diagnosed in the tail and the curve in dashes is proportional to 1/(time), but converges to $c^*=1.6<\bar{c}$. Note that even though there is a singularity behind the front the behavior of the local speeds diagnosed in the tail is continuous and algebraic.

the solution is forced to approach the inception of the strongly stable manifold. It is therefore driven to approach the saddle point $-u_s$ and form a $c=0$ heteroclinic connection between u_s and $-u_s$. Once the zero speed connection is established, the solution can approach zero along the strongly stable manifold, forming a SH connection from the negative side.

This sequence of events is illustrated in Fig. 12. The solid curve is a time slice of the developing front, plotted in phase space. The dashed curve is the SH connection from $-u_s$ to zero, and the curve with dashes and dots is the motionless connection between u_s and $-u_s$. In converging to the SH connection, the solution must leave the vicinity of the oscillatory fronts, but this manifold of solutions still plays an organizing role. The actual solution undergoes such contortions because its asymptotic behavior is attempting to converge along the manifold of fronts, while its topology requires it to pay the price of connecting to $-u_s$ first. The tail of the front acts continuously; the local speeds depicted in Fig. 11 behave quite nicely, regardless of the contortions of the solution. This indicates that our argument about maximal growth rates in Sec. IV is correct. The dynamics of the tail, getting pulled in the direction of maximum temporal growth, determines the behavior of the rest of the front.

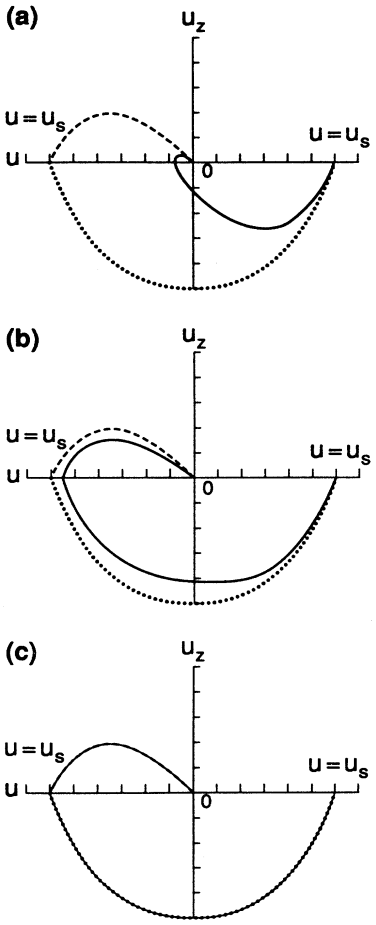

FIG. 12. (a) Phase space for μ-0.64 and $c_0=1.0$. The solid curve is the initial condition. The dashed curve is the nonlinear WTC solution on the negative side and the dash-dotted curve is the zero speed heteroclinic connection between the two nonzero fixed points. (b) Same as (a). The solid curve is the PDE solution plotted at time 5. Note how the trajectory has expanded toward the zero speed trajectory (dash-dotted) and has not yet been able to approach the SH trajectory (dashed). (c) Final state for the initial condition in (a). The solid curve is the actual solution, the dashed curve is the WTC solution, and the dash-dotted curve is the heteroclinic connection between the finite-amplitude fixed states.

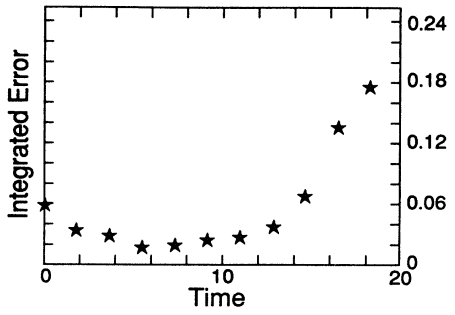

FIG. 13. Distance between transients and the manifold of front solutions according to the norm D. The initial condition is oscillating and on the manifold of fronts with speed $c_0=1.2$ for $\mu=0.64$. The distance between the transient and the manifold of fronts stays small until the local speed makes the jump to $\bar{c}$. At this point the ODE solver is unable to resolve the nonlinear front, and consequently the error seems large. The transient behavior of the norm D indicates that even when the nonlinear front is the asymptotic state the oscillating fronts attract and organize convergence.

To demonstrate that the oscillatory fronts still play an organizing role in convergence, Fig. 13 is a plot of the integrated error as fronts are in the process of converging

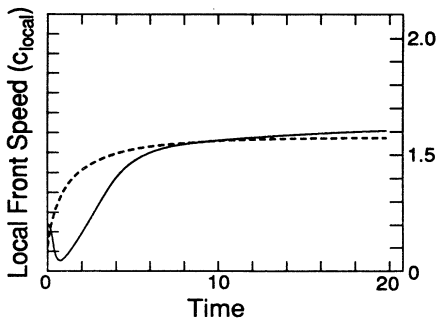

FIG. 14. Local front speeds for $\mu=0.64$ and $c_0=1.2$. The solid curve is local front speed diagnosed in the tail and the curve in dashes is proportional to 1/(time) and converges to $c^*=1.6<\bar{c}$. As before, convergence is algebraic and from below, even though the nonlinear front is the asymptotic state.

to the front with speed $\tilde{c}$. The parameter values are the same as for the previous run depicted in Figs. 11 and 12. The speed of the initial condition was chosen to be $c_0=1.2$. Figure 14 is a plot of c_{local} against time for this experiment. Note that when the transient has speed $c_{\text{local}}<c^*$ the distance between it and the oscillatory fronts is small. As the speed jumps to $\tilde{c}$, the error grows large (because the ODE solver can not reproduce the SH connection). As before, when we relax the restriction on positivity, the dynamically relevant portion of the manifold of fronts is the portion with speeds $c<c^*$, corresponding to oscillatory solutions.

VI. LIAPUNOV ARGUMENT FOR STABILITY

From an analysis of the tails of the various fronts and their corresponding temporal growth rates, we have quantified when the linear and nonlinear fronts are asymptotically preferred. We will now attempt to produce and justify these results in the context of Liapunov functionals. Unfortunately, when no minima exist for the Liapunov functional, it is not at all clear how the functional is useful. However, proceeding with the ansatz that locally in time the Liapunov functional will always develop along the direction of its highest derivative, we make an initial attempt to use the Liapunov functional in the context of fronts. Our arguments apply to (6), and could easily be written down for (3). Similar results apply for both Eqs. (3) and (7). Due to the absence of a Liapunov functional in (7) these arguments do not apply, even though the behavior of fronts in this equation obeys the same sort of laws. We intend the Liapunov functional argument presented here to illustrate the idea that the most unstable direction leaving zero defines a dominant front. However, this idea has broader relevance than the Liapunov functional argument, which is simply fortuitous for illustrating our idea in the context of (6).

Define the function

$$G(u,x)=u_x^2-\mu u^2-\tfrac{1}{2}u^4+\tfrac{1}{3}u^6$$

and the functional

$$F[u]=\int_0^\infty G(u,x)dx \ .$$

If u is a solution to (6), then

$$\begin{aligned}F_t[u]&=2\int_0^\infty u_x u_{xt}-u_t(\mu u+u^3-u^5)dx\\&=2u_x u_t|_0^\infty-2\int_0^\infty u_t^2dx \ .\end{aligned}$$

If u is a front solution, then we have shown earlier that as $z\to-\infty$ the solution $u-u_s\sim\exp(\eta z)$ with $\eta>0$ and determined at the beginning of Sec. V. Hence, for a front solution eventually we have

$$u_x(0)\sim e^{-c\eta t} \ ,$$

and hence the error we make neglecting boundary contributions to F_t become small exponentially in time. For fronts, then, we will write

$$F_t[u]=-2\int_0^\infty u_t^2dx=-2c^2\int_0^\infty u_z^2dx \ . \tag{33}$$

For fronts, the size of the integral in (33) depends monotonically on c. To see this recall the energy formulation of the ODE, (28). Integrating this equation gives

$$\begin{aligned}-2c\int_0^\infty u_z^2dx&=(u_z^2+\mu u^2+\tfrac{1}{2}u^4-\tfrac{1}{3}u^6)_0^\infty\\&=-(\mu u_s^2+\tfrac{1}{2}u_s^4-\tfrac{1}{3}u_s^6)\\&=u_s^4(\tfrac{1}{2}-\tfrac{2}{3}u_s^2)=G(u_s,0) \ .\end{aligned} \tag{34}$$

Using (34), we can write the time dependence of the functional as

$$F_t[u]=cG(u_s,0) \ . \tag{35}$$

$G(u_s,0)$ is a negative constant that is independent of c.

We make the ansatz that stable fronts minimize F_t, while accessible fronts are minima in directions perpendicular to the manifold of fronts. The properties of a gradient flow ensure that solutions seek local minima of F, but as we have already shown these minima depend on time. In this case we suggest that the dominant solution is the one which minimizes F_t; of all the possible ways that F can grow more negative, the dominant solution chooses the fastest. We illustrate this idea with what we already know about the stability of fronts. Let $c^\dagger$ and $u^\dagger$ be the front speed and corresponding front which minimizes F_t in the set of accessible fronts. Equation (35) shows that $c^\dagger$ must be the maximum front speed from the set of observable speeds, which we determined in Sec. V. Thus $c^\dagger$ is either c^* or $\tilde{c}$, whichever is greater.

Let

$$U(x,t)=U\left[x-c^\dagger t+\epsilon\int vdt\right] \ ,$$

and ask that U satisfies (24) when c is replaced by $c^\dagger-\epsilon v(t)$. The dependence of v on time is not determined except insofar as it must be positive since $c^\dagger$ is maximal. We can Taylor expand F_t in c and t to determine its behavior for U,

$$\begin{aligned}F_t[U]=c^\dagger G(u^\dagger,0)+t&\left[c^\dagger\frac{\partial G}{\partial t}(u^\dagger,0)+\epsilon v'(t)G(u^\dagger,0)\right]\\&+\epsilon v\left[G(u^\dagger,0)+c^\dagger\frac{\partial G}{\partial C}(u^\dagger,0)\right]+\mathcal{O}_{\text{HO}} \ ,\end{aligned} \tag{36}$$

where $\mathcal{O}_{\text{HO}}$ represents higher-order terms. In (36), $(\partial/\partial t)G(u^\dagger,0)\to0$ exponentially, and can therefore be neglected. Since $G(u^\dagger,0)$ is independent of c, the partial with respect to c vanishes; and since $c^\dagger$ minimizes F_t in the accessible set

$$\begin{aligned}G(u^\dagger,0)\{c^\dagger+\epsilon[tv'(t)+v]+\mathcal{O}_{\text{HO}}\}&=F_t[U]>F_t[u^\dagger]\\&=c^\dagger G(u^\dagger,0) \ .\end{aligned}$$

Hence

$$G(u^\dagger,0)(tv'+v)>0 \ ,$$

and since $G(u^\dagger,0)<0$

$$tv'(t)+v(t)<0 \ .$$

This shows that $v(t)\rightarrow 0$ more quickly than

$$\frac{v_0 t_0}{t_0+t} ,$$

and therefore an unstable front accelerates through the class of oscillatory front solutions, evolving to approach the front $u^\dagger$ with speed $c^\dagger$. This result is in agreement with van Saarloos, who actually produces a more exact result (although it is not connected explicitly with the transient oscillatory continuum of fronts).

At this juncture it is reasonable to ask why this argument does not apply to the over-damped fronts. Should not (35) imply that the greater the speed of a front, the greater its stability? In Sec. IV we assert that the overdamped fronts in the ODE are inaccessible in the PDE, while the oscillatory fronts are algebraically unstable along the observable manifold. The continuum of nonmonotonic fronts therefore lies at the bottom of a valley in function space, and the flow F_t runs down the sides of this valley to the manifold of solutions. The analysis presented in this section shows that the valley floor is slightly tilted in the direction of maximum speed. Solutions on the valley floor approach the maximum nonmonotonic speed $c^\dagger = c^*$ or $\bar{c}$.

The overdamped $c > c^\dagger$ fronts are unreachable in the PDE; a structural deviation from a solution to (24) with $c > c^\dagger$ is unstable, even though the exact solution is stable. In particular, a $c > c^\dagger$ front that is truncated in the tail, such as we used for numerical initialization in Sec. V is unstable. This illustrates that in function space the overdamped solutions are saddle points of the flow F_t, and therefore can not be reached by solutions to the PDE. To illustrate this structure in function space, we need to understand the behavior of the functional F_t for perturbations near the manifold of fronts. In particular we will consider F_t for perturbations that may be parametrized by c; we will consider perturbations by the companion mode in the linear dispersion relation (31).

Let $u(z=x-ct)$ be a front solution. We know that asymptotically in the tail

$$u \sim e^{\lambda_+ z} ,$$

where

$$\lambda_\pm = \tfrac{1}{2}[-c \pm (c^2-4\mu)^{1/2}] .$$

Here $e^{\lambda_- z}$ is the "companion mode" we refer to above. Let

$$\hat{u} = u + \epsilon H(z-z_0) e^{\lambda_-(z-z_0)} ,$$

so that the solution u is perturbed by the companion mode in the tail and z_0 is chosen so that it is in this asymptotic region. The perturbation moves at the same speed as the front, so that we can evaluate the functional in a traveling frame of reference

$$F_t[\hat{u}] = cG(u_s,0) - 2\epsilon c^2 \int_{z_0}^{\infty} (\lambda_+^* \lambda_- e^{\lambda_+^* z} e^{\lambda_-(z-z_0)} + \lambda_-^* \lambda_+ e^{\lambda_+ z} e^{\lambda_-^*(z-z_0)}) dz . \tag{37}$$

In Eq. (37) the asterisk denotes the complex conjugate and the integral is evaluated to leading order in ϵ. To continue we must divide the analysis into three parts, depending on $c > \bar{c}$, $c < c^*$ or $c^* < c < \bar{c}$.

(i) $c > \bar{c}$. Here $\lambda_\pm$ are real, and hence

$$F_t[\hat{u}] = cG(u_s,0) + 4\epsilon c^2 e^{\lambda_+ z_0} \frac{\lambda_+ \lambda_-}{\lambda_+ + \lambda_-} . \tag{38}$$

From the definition of $\lambda_\pm$

$$\lambda_+ \lambda_- = \tfrac{1}{4}(c^2 - c^2 + 4\mu) = \mu$$

and

$$\lambda_+ + \lambda_- = -c .$$

Thus we have

$$F_t[\hat{u}] = cG(u_s,0) - 4\epsilon c \mu e^{\lambda_+ z_0} < cG(u_s,0) = F_t[u] .$$

For the overdamped fronts, adding a perturbation that moves at the same speed but has steeper exponential dependence lowers the energy of the front. The properties of the gradient flow dictate that infinitesimal perturbations of this kind force u to move to a lower-energy state. Therefore the overdamped fronts are saddles in function space.

(ii) $c < c^*$. Here $\lambda_- = \lambda_+^*$, and therefore

$$F_t[\hat{u}] = cG(u_s,0) + 4\epsilon c^2 \left[\frac{\lambda_+^2}{2\lambda_+} e^{\lambda_+ z_0} + \frac{\lambda_-^2}{2\lambda_-} e^{\lambda_- z_0} \right] . \tag{39}$$

In this case the companion mode and the tail of the front have the same spatial structure; only the phases differ. Perturbing with the same phase as the front is equivalent to merely translating the front, while perturbing out of phase may change the solution. By translational invariance, we may assume the phase of u to be zeroed when $z_0 = 0$. We must therefore choose

$$z_0 = \frac{(2n-1)\pi}{\kappa} ,$$

with n an integer and $\kappa = \mathrm{Im}(\lambda_+)$, to investigate the energy of an out-of-phase perturbation. With z_0 chosen as above, (39) becomes

$$\begin{aligned} F_t[\hat{u}] &= cG(u_s,0) + 4\epsilon c^2 \,\mathrm{Re}[\lambda_+ e^{\lambda_+ z_0}] \\ &= cG(u_s,0) + 2\epsilon c^2 e^{-cz_0/2} \,\mathrm{Re}\{(-c+i\kappa)[\cos(\kappa z_0) + i \sin(\kappa z_0)]\} \\ &= cG(u_s,0) + 2\epsilon c^3 e^{-cz_0/2} > F_t[u] . \end{aligned}$$

The energy of the underdamped fronts is lower than the energy of the perturbed front, which must therefore decay to the unperturbed front.

(iii) $c^* < c < \bar{c}$. Here the calculation is the same as the case $c > \bar{c}$ insofar as $\lambda_\pm$ are real. The difference is that the asymptotic behavior of u changes signs. As we demonstrated in Sec. V, these fronts are forced to converge from the $u < 0$ side by the topology of the SH connection. Then

$$u \sim -e^{\lambda_+ z} ,$$

and therefore we may rewrite (38)

$$F_t[\hat{u}] = cG(u_s,0) - 4\epsilon c^2 e^{\lambda_+ z_0} \frac{\lambda_+ \lambda_-}{\lambda_+ + \lambda_-} .$$

This gives

$$F_t[\hat{u}] = cG(u_s,0) + 4\epsilon c\mu e^{\lambda_+ z_0} > cG(u_s,0) = F_t[u] .$$

Our analysis suggests that for $c < c^\dagger$ the manifold of fronts is attracting, while for $c > c^\dagger$ it is repelling. This result vindicates van Saarloos's contention that $c = c^\dagger$ (whether $c^\dagger = \bar{c}$ or c^*) corresponds to a front with marginal stability. Since it occurs at the boundary between attracting and repelling states on the manifold of front solutions to the ODE, $c^\dagger$ is marginal. However, the analysis here is based on the ansatz that the flow in function space minimizes the functional F_t, which is analogous to assuming that the flow follows the direction of maximum stability whenever possible. Although this is reasonable, it is certainly not yet proven. In this context it makes our results very suggestive, but by no means rigorous.

We should note that our prediction of algebraic convergence of front speeds from below agrees with van Saarloos's more precise estimate of algebraic convergence to the linear marginal front speed c^*. He also asserts that convergence to the SH front speed $\bar{c}$ should be exponential. While this is not obvious from the above analysis, it is a reasonable conclusion given the fact that solutions near fronts with speed $c > c^\dagger$ are exponentially unstable to the companion mode in the PDE dispersion relation. Algebraic convergence is allowed when fronts are able to converge through the manifold of oscillatory front solutions. If we start with a solution to the ODE (24) with speed not in the continuum of potentially stable speeds, the convergence to the maximal speed (either $\bar{c}$ or c^*) should be exponential, since these solutions break down via the growth of an exponentially unstable mode.

We have chosen to illustrate our maximum temporal growth principal with the Liapunov functional for Eq. (6). This principal applies in equations like (7), even when a Liapunov functional does not exist. In time, the fact that zero is unstable forces the PDE to asymptotically choose the maximum growth mode, which then develops into a front connection. In the frame of reference of a front, this corresponds to the steepest asymptotic decrease of the envelope of a front. In (7) fronts speeds converge to the larger of c^* or $\bar{c}$ because these give the maximum departure from zero. The Liapunov functional allows us to make this argument more concrete in the case of (6), but the lack of a Liapunov functional in (7) does not change the force of our approach.

VII. VAN SAARLOOS'S ARGUMENT

van Saarloos exhaustively discussed the front problem for his version of the equation (6) and heuristically deduced the correct behavior. Since parts of this paper reproduce his results, we should summarize his arguments in the framework we have presented and show how our analysis compares with his.

Any front solution to (6) must decrease to zero as $x \to \infty$, and so the tail of the front must obey the linear equation

$$u_t = \mu u + u_{xx} . \tag{40}$$

Consider the behavior of a linear mode

$$u \sim \exp[i(\omega - i\sigma)t + i(k - i\lambda)z] ,$$

where $z = x - ct$ and c is the front speed. For this mode to be part of a persistent front, it must have zero temporal growth in a frame traveling with speed c. Thus $\sigma = 0$. This gives the dispersion relation

$$i\omega = \mu + ic(k - i\lambda) - (k - i\lambda)^2 . \tag{41}$$

For $\omega = 0$, we must have $k = 0$ and therefore

$$\lambda = \tfrac{1}{2}[-c \pm (c^2 - 4\mu)^{1/2}] . \tag{42}$$

This is the branch (λ real) of asymptotic behavior considered by van Saarloos when he draws the $c(\lambda)$ curve in Fig. 15. Every front in this class is nonoscillatory and has velocity $c \geq c^* = 2\sqrt{\mu}$.

For each front with speed c,

$$u(z) \sim K_1(c) e^{\lambda_1(c) z} + K_2(c) e^{\lambda_2(c) z} \tag{43}$$

as $x \to \infty$, with $0 > \lambda_1(c) > \lambda_2(c)$. van Saarloos makes the statement that if $K_1(c) \neq 0$, the asymtotic form of the front is dominated by the exponential decrease $\lambda_1(c)$, since the other part of the linear combination decreases

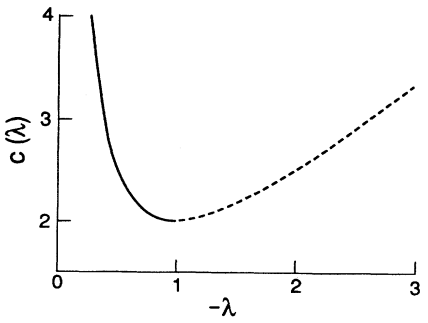

FIG. 15. van Saarloos's dispersion relation. The solid branch is the branch of relevant asymptotic behavior, and the dashed branch is the branch to which fronts on the solid branch are unstable in the PDE. The dispersion relation was plotted using the parameter value $\mu = 1$.

exponentially more rapidly in z. Thus van Saarloos only considers the branch of Fig. 15 to the left of $-\lambda=-\mu$ (marked A in Fig. 15); the portion to the right (labeled B) does not correspond to an asymptotic approach to zero. van Saarloos's observation is exactly equivalent to our assertion that the front trajectory in the ODE (24) generically approaches zero along the weakly attracting eigendirection of zero (as illustrated in Figs. 1 and 2). These overdamped ($c>c^*$) solutions, while reasonable in the context of the ODE, are not accessible solutions to the PDE, starting from compact support.

If we substitute $\sigma=-c\lambda$ in (42), corresponding to looking at the temporal growth of a mode λ viewed in a stationary frame of reference, the dispersion relation for nonoscillatory solutions becomes

$$\sigma=\mu+\lambda^2 .$$

In a stationary frame the time growth of the tail becomes

$$u(z)\sim K_1(c)e^{\sigma_1(c)t}+K_2(c)e^{\sigma_2(c)t} , \tag{44}$$

with

$$\sigma_1<\sigma_2 .$$

The temporal mode with growth rate σ_2 grows exponentially faster than the mode with growth rate σ_1, and thus the overdamped fronts on the left-hand branch of Fig. 15 are inaccessible from compact support initial conditions because modes on the right-hand branch, which (in general) are not connected to fronts, grow exponentially faster in a stationary frame of reference. The stable, overdamped branch of fronts are unobservable in these circumstances. Oscillatory fronts, while unstable, are approachable and therefore dynamically relevant. van Saarloos and earlier authors have not considered the oscillatory fronts because they are not positive and not stable, while they were looking for positive asymptotic states. But it is precisely the transient properties of the unstable oscillatory fronts which allows us to understand the mechanics of convergence when positivity is not maintained.

For $c<c^*$, (42) gives

$$\lambda=-\frac{c}{2},\quad k=\pm\tfrac{1}{2}(4\mu-c^2)^{1/2},\quad \omega=0 .$$

With $c<c^*$, zero becomes a spiral note in the ODE and there is no stronger or weaker eigendirection. Thus σ_1 and σ_2 in (44) are the same and the oscillatory fronts are observable in the PDE, or at least they are not unstable to an exponentially growing companion mode. Therefore the continuum of observable fronts in the PDE have speeds in $[0,2\sqrt{\mu}]$.

There is one other potentially accessible front. When the SH connection depicted in Fig. 2(b) is possible, it is nongeneric in the ODE. As van Saarloos points out, the SH front with speed $\tilde{c}$ has

$$K_1(\tilde{c})=0 .$$

Therefore the SH front is not unstable to the mode with growth rate σ_2; it *is* the mode with growth rate σ_2.

van Saarloos argues that the profile with the most rapid exponential drop-off (smallest $\lambda<0$) is the most stable front. We agree, and would like to cast his shape arguments in our framework. Returning to the functionals F and F_t above, recall

$$F_t(u)=-2\int_0^\infty u_t^2 dx .$$

If we evaluate F_t for a front solution, the maximal contribution to the integral is from the tail. The portion of the integral over which $u\to u_s$ has $u_t\sim 0$ and therefore makes negligible contribution. The transition from $u=u_s$ to u small occurs over a small region, and therefore it is reasonable to write

$$F_t(u)\sim -2c^2\lambda\int_{z_0}^\infty e^{2\lambda z}dz , \tag{45}$$

where

$$u\sim e^{\lambda z}$$

is the dominant asymptotic behavior of the front with speed c, and z_0 is an (arbitrary) point in the traveling frame where the solution becomes linearly determined. The linear dispersion relation for the ODE gives

$$-c\lambda=\mu+\lambda^2 ,$$

and thus the integral (45) is dominated by the front with largest λ^2, or most rapid decrease in its exponential envelope. Since $\sigma=-c\lambda$ is the temporal growth rate of a front in a stationary frame, we may say that F_t is minimized by a frontal solution with maximum temporal growth at a point.

VIII. CONCLUSION

The results about asymptotic front speed presented in this paper are not new; van Saarloos's rule that maximum asymptotic spatial decrease equates to maximum stability is certainly correct. Our contribution is an alternative, and perhaps more heuristic, understanding of why this must be so. We have presented explanations for why and demonstrated numerically that the continuum of observable fronts lies below the marginal speed c^* in the presence of nonpositive perturbations. This is directly opposed to what is suggested by the analysis of previous authors, whose stability results might suggest that overdamped fronts could be observable from compact support initial conditions. To understand the interaction between the PDE and the traveling frame ODE it gives rise to, we must understand that an observable front occurs only when the asymptotic behavior of a perturbation in the PDE and a solution to the ODE concur.

We have shown that van Saarloos's stability rule is also the Dee and Langer argument for asymptotic front speed. That is, the propagating behavior of the most unstable mode which allows a front connection describes the asymptotic front behavior. The mode with maximum growth rate at a stationary point is the mode to which all compactly supported initial conditions are unstable; the front arising from the mode is the asymptotic front. Kolmogorov's stationary phase argument is a mathematical statement of just this idea. Where Kolmogorov's argument fails to choose the asymptotic front, it does so be-

cause the asymptotic front has speed outside the generic continuum of fronts. Thus the method of steepest descent, which depends on maximization of growth rate via a derivative argument, does not apply.

Using a Liapunov functional for the real equation, we have suggested that the dynamic competition of fronts evolving from compact support can also be understood as the Liapunov functional's flow in function space. It is an unproven but reasonable ansatz that the Liapunov functional develops by maximizing its time derivative, and this leads naturally to a restatement of the selection criterion based on maximum temporal growth rate. The fact that there is no Liapunov functional for CGL-type equations does not make the selection criterion less valid. Intuitively it is clear that the maximum temporal growth rate whose spatial dependence corresponds to a trajectory in the ODE must be the stable front. Preliminary numerical results for (7) indicate transition behavior from the WTC to the marginal fronts as μ passes the critical value found in Sec. III. Proof cannot be far behind.

The last result that deserves comment is that WTC fronts are stable solutions in what would be the most physical parameter regime of (7). Because the amplitude of hydrodynamics waves scales algebraically with the change in a stress parameter near criticality, an equation like (7) can only be physically relevant in a regime of small $|\mu|$. This is precisely where WTC fronts predominate. This paper was not intended to explore characteristics of integrability in nonintegrable equations. Rather the point of this paper is to show that the special WTC solutions, which are known to have certain analytic properties, are also possessed of stability properties in the most physical regime of parameters as well as topological properties in phase space. Connecting these three concepts mathematically will be the basis for future work.

The results in this paper are very suggestive springboards for future work. As we have pointed out in the course of this paper, the same path may be followed for Ginzburg-Landau-like equations. However, when the finite amplitude state at $-\infty$ is a time-dependent plane wave, the potential instability of the plane wave may interact with the selection of the front speed. We have shown that our results fit neatly into a Liapunov functional argument where such an argument exists. By extension the same sorts of things must be happening for small β and γ in (7). When solutions converge to an integrable trajectory, it suggests that a conservation law is trying to be obeyed, which in turn suggests that *something* is being minimized. Thual and Fauve [17] have shown that in (7) with $\beta=\gamma=0$ there is also a branch of solitary-wave states with large wave number. In our Liapunov model, these wave states are a branch where the kernel of the free energy is identically zero. How does this perturb to complex parameters, and how do these states compete with the linear and nonlinear fronts? When complex parameters are added, can the Liapunov functional still be used to describe the oscillation and stability of the new states? In two space dimensions, the convergence of fronts to the nonlinear front will leave behind a line singularity in wave number. Is this a way to seed spiral waves starting with plane-wave states? Also, in higher dimensions what is the nature of special integrable solutions, and how does their strong spatial structure organize the behavior of more generic solutions? The interaction between generic and nongeneric behavior, which we have described for the simple model (6) in this paper, may be a seed crystal for our understanding of many more complex systems.

ACKNOWLEDGMENTS

The authors thank the Arizona Center for Mathematical Sciences (ACMS) for support. ACMS is sponsored by AFOSR Contract No. FQ8671-9000589 (AFOSR-90-0021) with the University Research Initiative Program at the University of Arizona. The work herein was also supported by the National Science Foundation under Grant No. DMS 8801627 and the Graduate Research Board of the University of Maryland.

*Present address: Department of Math and Statistics, Utah State University, Logan, UT 84321.

[1] A. Kolmogorov, I. Petrovsky, and N. Piscounov, Bull. Univ. Moscow, Ser. Int., Sec. A **1**, 1 (1937).
[2] A. C. Newell and J. A. Whitehead, in *Proceedings of the International Union of Theoretical and Applied Mechanics Symposium on Instability of Continuous Systems, Herrenalb, 1969,* edited by H. Leipholz (Springer-Verlag, Berlin, 1971), pp. 284–289.
[3] A. C. Newell, Lect. Appl. Math. **15**, 157 (1974).
[4] K. Stewartson and J. T. Stuart, J. Fluid Mech. **48**, 529 (1971).
[5] A. C. Newell and J. A. Whitehead, J. Fluid Mech. **38**, 279 (1969).
[6] L. A. Segel, J. Fluid Mech. **38**, 203 (1969).
[7] G. Dee and J. S. Langer, Phys. Rev. Lett. **50**, 383 (1983).
[8] R. A. Fisher, Ann. Eugenics **7**, 355 (1937).
[9] K. Nozaki and N. Bekki, Phys. Rev. Lett. **51**, 2171 (1983).
[10] D. G. Aronson and H. F. Weinberger, Adv. Math. **30**, 33 (1978).
[11] E. Ben-Jacob, H. Brand, G. Dee, L. Kramer, and J. S. Langer, Physica D **14**, 348 (1985).
[12] W. van Saarloos, Phys. Rev. A **37**, 211 (1988).
[13] W. van Saarloos, Phys. Rev. A **39**, 6367 (1989).
[14] F. Cariello and M. Tabor, Physica D **39**, 77 (1989).
[15] C. K. R. T. Jones, T. M. Kapitula, and J. A. Powell, Proc. R. Soc. Edinburgh A **116**, 193 (1990).
[16] A. Bernoff, Physica D **30**, 363 (1988).
[17] O. Thual and S. Fauve, Phys. Rev. Lett. **64**, 282 (1990).